Carbon nanofiber based electrochemical biosensors: A review

Jianshe Huang, Yang Liu and Tianyan You*

Received 17th December 2009, Accepted 6th January 2010
First published as an Advance Article on the web 25th January 2010
DOI: 10.1039/b9ay00312f

Carbon nanofibers (CNFs), a novel carbon nanomaterial, have the similar conductivity and stability to carbon nanotubes (CNTs). The main distinguishing characteristic of CNFs from CNTs is the stacking of graphene sheets of varying shapes, producing more edge sites on the outer wall of CNFs than CNTs, which can facilitate the electron transfer of electroactive analytes. The unique chemical and physical properties make CNFs exceptional candidates for electrode materials and promising candidates as immobilization substrates. This review is an attempt to give an overview on electrochemical biosensors based on CNFs and their various applications. We discussed the application of CNFs as electrode material in electroanalysis, as well as their functionalization and surface immobilization. Vertically aligned carbon nanofibers (VACNFs) as substrates for the immobilization of biological molecules have also been discussed.

1. Introduction

Carbon materials possess suitable properties for the design of electrodes used in electroanalytical chemistry because of their relatively wide potential windows in aqueous media, low cost, and relative chemical inertness in most electrolyte solutions. There are several available microstructures of carbon materials, such as graphite, glassy carbon, carbon fiber, nanotubes, amorphous powders, and diamond.[1] With the continuous progress of nanotechnology in material science, carbon nanomaterials, especially carbon nanotubes (CNTs) and carbon nanofibers (CNFs), have attracted considerable attention in electroanalysis and biosensing. Since their discovery in 1991,[2] study on the properties and applications of CNTs has rapidly increased. The functionalization and application of CNTs in electroanalysis have been extensively reviewed in recent years.[3–7] The studies demonstrated that CNTs can significantly enhance the electrochemical reactivity of important biomolecules and can promote the direct electron-transfer reaction of proteins. Additionally, CNT-modified electrodes can also alleviate the surface fouling effects. These properties make CNTs extremely attractive for a wide range of electrochemical biosensors.

CNFs have cylindrical nanostructures with different stacking arrangements of graphene sheets, such as stacked platelet, ribbon or herringbone (Fig. 1).[8] They have lengths in the order of micrometres, while their diameter varies between some tens of nanometres up to several hundreds of nanometres. The mechanical strength and electric properties of CNFs are similar to that of CNTs while their size and graphite ordering can be well controlled.[9] The primary distinguishing characteristic of CNFs from nanotubes is the stacking of graphene sheets of varying shapes, producing more edge sites on the outer wall of CNFs than CNTs.[10] The presence of more edge plane defects may facilitate the electron transfer of electroactive analytes.[11] Additionally, CNFs are unique in the fact that their whole surface area can be activated. Activation of CNFs with nitric acid or electrochemical oxidation can produce a range of oxygen-containing groups without degradation of the structural integrity of their backbones.[12] Since CNFs have a much larger functionalized surface area compared to that of CNTs, the surface-active groups-to-volume ratio of these materials is much larger than that of the glassy-like surface of CNTs. These properties mean CNFs can be ideal immobilization matrixes for biomolecules, at the same time they can transmit electrochemical signals acting as transducers.

However, the application of CNFs has been mainly focused on catalyst supports,[8,13] gas-storage systems,[14] polymer reinforcements,[15] probe tips,[16] and many others in the past decades. Until recently, CNFs have been extensively used for biosensor

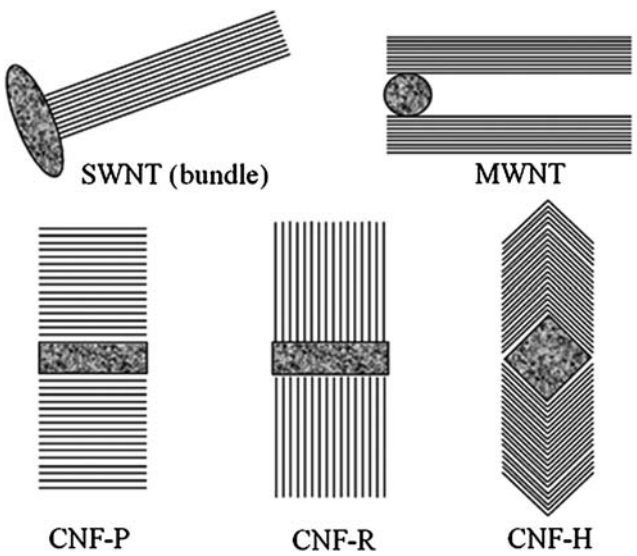

Fig. 1 Schematic representation of different stacking shapes of graphene sheets of CNT and CNF. CNF–P: platelet carbon nanofiber; CNF–R: ribbon-like carbon nanofiber; CNF–H: herringbone carbon nanofiber (reproduced with permission from Ref. 8).

State Key Laboratory of Electroanalytical Chemistry, Changchun Institute of Applied Chemistry, Chinese Academy of Sciences, Changchun, 130022, P.R. China. E-mail: youty@ciac.jl.cn; Fax: +86-431-85262850; Tel: +86-431-85262850

development because of their unique physical and chemical properties (*e.g.*, good electrical conductivity, high surface area, biocompatibility, inherent and induced chemical functionalities, and ease of fabrication).[7,9,17–21] The studies demonstrated that CNFs could be used as ideal immobilization substrates for biomolecules and as signal transducers. Additionally, vertically aligned carbon nanofibers (VACNFs), where CNFs are grown perpendicularly to the substrate, are emerging as useful materials for applications such as chemical sensing/biosensing. However, no review on the application of CNFs in the construction of biosensors except a brief overview has been reported.[7] Therefore, in the present review we summarized recent advances in the use of CNFs and VACNFs for biosensing application. This review mainly highlights the design, performance characteristics, and applications of CNF-based electrochemical biosensors, as well as the functionalization methods of VACNFs.

2. Carbon nanofiber-based electrochemical biosensors

2.1. CNF-modified electrodes for the direct detection of small molecules

Marken and his co-workers firstly studied the voltammetric behaviors of CNF composite electrodes.[22,23] Nanocomposite electrodes made of carbon nanofibers and paraffin wax were characterized and investigated as novel substrates for metal deposition and stripping processes. They also explored the electrochemical properties of CNF–ceramic composite electrodes,[24,25] and CNF–polystyrene composite electrodes.[26] Maldonado and Stevenson directly prepared carbon nanofiber electrodes by pyrolysis of iron(II) phthalocyanine on nickel substrates, and investigated the electrochemical behavior and stability of CNF electrodes as oxygen reduction catalysts.[12,27] They found that the disorder in the graphite fibers, the presence of exposed edge plane defects and nitrogen functionalities are important factors for influencing adsorption of reactive intermediates and enhancing electrocatalysis for O_2 reduction. Compared with nondoped CNF electrode, nitrogen-doped (*N*-doped) CNF electrode exhibited significant catalytic activity toward O_2 reduction at neutral to basic pH.

Similarly to CNTs, CNFs as catalytic materials have attracted considerable attention in electrochemical sensing. In order to improve the dispersity of CNFs, it is common to treat them by harsh oxidation or by selecting appropriate solvent. Arvinte and coworkers studied the performance of CNF-modified glassy carbon (CNF–GC) electrode in the direct electrochemical detection of NADH.[28] CNFs were dispersed into CH_3CN using an ultrasonic bath and then used to modify GC electrodes. A decrease of the oxidation potential of NADH by more than 300 mV was observed at CNF–GC electrode (0.32 V) comparing with a bare glassy carbon electrode (0.6 V). This sensor offered a detection limit of 11 μM NADH and a fast response time of 3 s.

Ju's group did a great deal of excellent works on the CNF based electrochemical biosensors. They used CNF-modified GC electrode for highly sensitive flow injection detection of hydrogen peroxide.[18] CNFs were firstly treated with 30% HNO_3 and refluxed for 24 h at 140 °C. The presence of CNF dramatically decreased the overpotential for H_2O_2 reduction (Fig. 2A), which

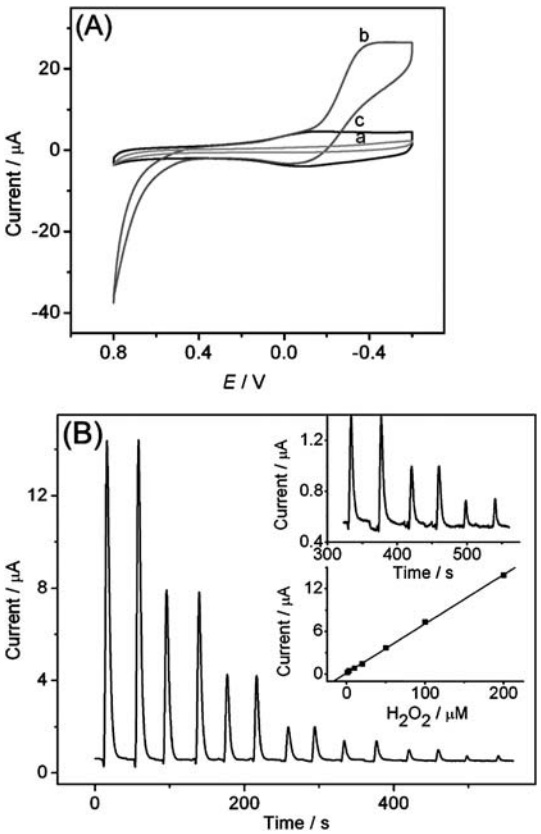

Fig. 2 (A) Cyclic voltammograms of 5.0 mM H_2O_2 at bare (a) and CNF-modified GCE (b) in pH 7.0 PBS, and the CNF-modified GCE in pH 7.0 PBS (c). Scan rate: 0.01 V s^{-1}. (B) Flow injection analysis with successive injections of 200, 100, 50, 20, 10, 3.0 and 1.0 μM H_2O_2 (from left to right) into pH 7.0 PBS at flow rate of 2.0 mL min^{-1} at −0.3 V. Upper inset: amplified response curve for injections of 10, 3.0 and 1.0 μM H_2O_2; lower inset: linear calibration curve (reproduced with permission from Ref. 18).

allowed conveniently low-potential amperometric detection of H_2O_2. The CNF–GC electrode was used for flow injection detection of H_2O_2, and exhibited a wide linear range of concentration and low detection limit of 0.5 μM (Fig. 2B). Ascorbic acid (AA) and uric acid (UA) had no interference with the detection of H_2O_2. The high sensitivity was ascribed to the excellent catalytic activity of CNFs, produced by both the oxygen containing groups and the edge sites.

Different carbon nanostructures, such as fullerenes, CNTs and CNFs were used as doping materials in biosensor membranes, and the efficiency of these materials as transducers and mediators in amperometric sensors was evaluated.[29] The study demonstrated that CNT-modified electrodes have a very low overpotential for the oxidation of H_2O_2, but they have a significantly high background current. On the other hand, the thermal stability of CNFs is more suitable for highly stable and sensitive biosensor systems. Li *et al.* studied the effect of microstructure of CNFs on the electrochemical sensing of H_2O_2.[30] They prepared CNFs with three different microstructures, including platelet-carbon nanofibers (PCNFs), fish-bone-carbon nanofibers (FCNFs), and tube-carbon nanofibers (TCNFs). The results showed that PCNFs/GC electrode exhibited higher electrocatalytic activity for the oxidation of H_2O_2 than FCNFs/GC and

TCNFs/GC electrodes. The excellent performance of PCNFs/GC electrode likely resulted from the specific microstructure of PCNFs, which has a large edge-to-base ratio, large numbers of active edge sites and a very large working surface area.

Electrospinning has been actively exploited as a valuable and versatile method for generating long polymer fibers with the diameter ranging from tens of nanometres to several micrometres. Carbonization of electrospun polymer nanofibers could be used to prepare CNFs. Recently, CNFs have been successfully prepared by electrospinning techniques in our laboratory. Electrospun CNF-modified carbon paste electrode (CNF–CPE) was used for mediatorless detection of NADH (Fig. 3).[31] This electrochemical sensor showed low detection limits down to nmol L^{-1}-level, wide linear range and good selectivity for selective determination of NADH in the presence of AA. CNF–CPE was also employed for the simultaneous determination of dopamine (DA), AA and UA by using differential pulse voltammetry (DPV) method.[32] Three well-defined peaks with remarkably increased peak current could be achieved at the CNF–CPE. Low detection limits of 0.04 μM, 2 μM and 0.2 μM for DA, AA and UA were obtained.

Palladium nanoparticle-loaded carbon nanofibers (Pd/CNFs) were synthesized by the combination of electrospinning, reduction and carbonization processes.[33] The metallic Pd nanoparticles were well-dispersed on the surface or completely embedded into CNFs. Pd/CNF-modified electrode exhibited high electrocatalytic activities towards the reduction of H_2O_2 and the oxidation of NADH. For H_2O_2, the Pd/CNF-modified electrode displayed a wider linear range from 0.2 μM to 20 mM with a detection limit of 0.2 μM at −0.2 V, and the detection was free from interference from the coexisted AA and UA. In the case of NADH, the linear range at the Pd/CNF-modified electrode was from 0.2 μM to 716.6 μM with a detection limit of 0.2 μM at 0.5 V. The high sensitivity, wide linear range, good reproducibility, and the minimal surface fouling make this Pd/CNF-modified electrode a promising candidate for amperometric H_2O_2 or NADH sensors. Pd/CNFs modified electrode also displayed excellent electrocatalytic activities towards DA, UA and AA.[34] The oxidation overpotentials of DA, UA and AA were decreased significantly compared with those obtained at the bare electrode by 159 mV, 265 mV and 600 mV, respectively. Differential pulse voltammetry was used for the simultaneous determination of DA, UA and AA in their ternary mixture, and three well-defined voltammetric peaks were obtained (Fig. 4). The calibration curves for DA, UA and AA were obtained in the range of 0.5–160 μM, 2–200 μM, and 0.05–4 mM, respectively. The lowest detection limits (S N^{-1} = 3) were 0.2 μM, 0.7 μM and 15 μM for DA, UA and AA, respectively. With good selectively and sensitivity, the present method was applied to the determination of DA in injectable medicine and UA in urine sample, and satisfactory results were obtained. Very recently, we prepared Ni nanoparticle-loaded carbon nanofibers (NiCF) by using the similar method to that of Pd/CNF.[21] NiCF paste (NiCFP) electrode exhibited excellent electrocatalytic performance for the oxidation of glucose. The amperometric responses of the NiCFP electrode to glucose showed a linear range from 2 μM to 2.5 mM with the detection limit of 1 μM at the applied potential of 0.6 V. The proposed electrode, exhibited good resistance to surface fouling and high operational stability, could be used as promising nonenzymatic glucose sensor.

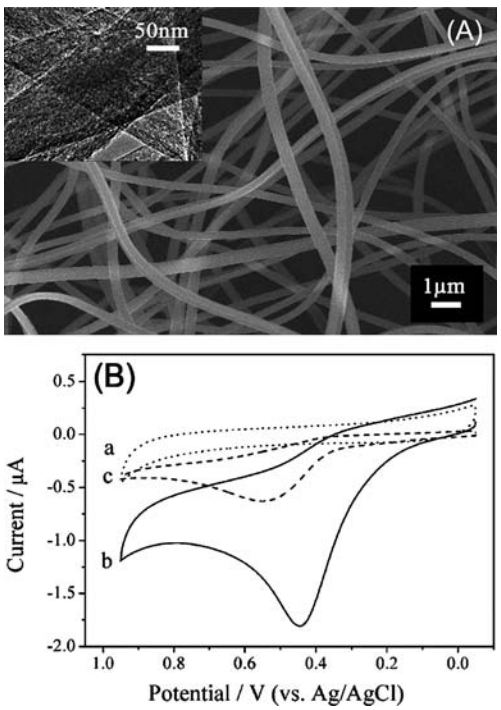

Fig. 3 (A) SEM image of electrospun CNFs. Inset shows TEM image of CNFs. (B) CVs of 0.1 M PBS (pH 7.0) a) plain and b) containing 1 mM NADH at the CNF–CPE; c) Corresponding CV of (b) with the CPE. Scan rate: 50 mV s^{-1} (reproduced with permission from Ref. 31).

2.2. CNF-based oxidase biosensors

Since CNFs have a much larger functionalized surface area compared to that of CNTs, the surface-active groups-to-volume

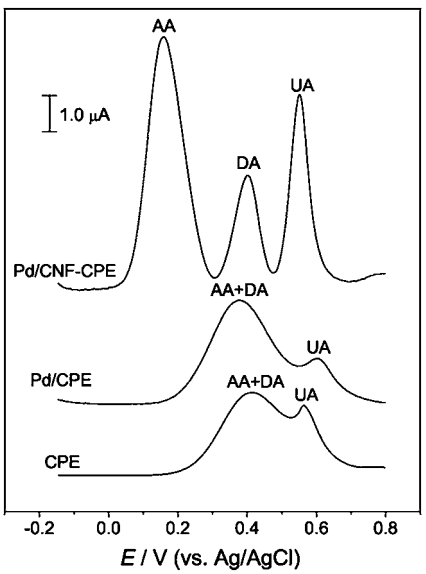

Fig. 4 DPVs at bare CPE, Pd/CPE and Pd/CNF–CPE in 0.1 M PBS (pH 4.5) containing 2 mM AA, 50 μM DA and 100 μM UA. DPV conditions: scan rate, 20 mV s^{-1}; amplitude, 50 mV; pulse width, 50 ms; pulse period, 200 ms (reproduced with permission from Ref. 34).

ratio of these materials is much larger than that of the glassy-like surface of CNTs.[9] This property, combined with the fact that the number and type of functional groups on the outer surface of CNFs can be well controlled, is expected to allow for the selective immobilization and stabilization of biomolecules such as proteins, enzymes, and DNA. Additionally, the high conductivity of CNFs seems to be ideal for the electrochemical transduction. Therefore, these nanomaterials can be used as scaffolds for the construction of electrochemical biosensors.

Vamvakaki *et al.* used three different types of CNFs and single-walled CNTs as well as graphite powder to prepare glucose biosensors and further compare their sensitivities and stabilities.[9] They firstly examined the number and type of the surface functional groups on CNFs by direct titration with NaOH or HCl solution. Because the total surface of CNFs could be functionalized, larger amounts of glucose oxidase (GOx) were immobilized on CNFs (Fig. 5), and then higher sensitivity could be obtained. The results demonstrated that CNFs are the best matrixes for immobilizing proteins and enzymes for biosensor development.

Ju's group employed soluble CNFs to prepare glucose amperometric biosensors based on catalytic reduction of dissolved oxygen.[19] A simple nitric acid treatment of CNF produced a large number of oxygen-rich groups on CNF surface, which significantly improved their solubility and dispersion ability. The membrane of CNF showed excellent stability and provided fast response to dissolved oxygen with a detection limit of 0.07 μM at −0.3 V. The proposed glucose biosensor could determine glucose ranging from 10 to 350 μM with detection limit of 2.5 μM, and the detection of glucose were free of interference from UA and AA. With a simple one-step electrochemical polymerization of thionine–CNF nanocomposite and alcohol oxidase (AOD), they also prepared poly(thionine)–CNF/AOD composite film-modified electrode.[35] Based on the excellent catalytic activity of the biocomposite film toward reduction of dissolved oxygen, a sensitive ethanol biosensor was proposed. This ethanol biosensor possessed excellent characteristics and performance, such as low detection limit, fast response and good stability. Recently, A hybrid nanocomposite of CNF with water-soluble iron(III) mesotetrakis(*N*-methylpyridinum-4-yl) porphyrin (FeTMPyP) was also used for preparation of highly sensitive ethanol biosensor.[36] The interaction between FeTMPyP and CNF *via* noncovalent π–π stacking resulted in the formation of CNF–FeTMPyP nanocomposite. Cyclic voltammograms of AOD/CNF–FeTMPyP modified GCE showed not only the redox peaks of FeTMPyP, but also the direct electrochemistry of AOD. The biosensor exhibited rapid and highly sensitive response to ethanol with a linear range from 2.0 μM to 112 μM.

2.3. CNF-based dehydrogenase biosensors

Coimmobilization of dehydrogenase enzymes and their NAD^+ cofactor to various solid electrodes are commonly employed for the detection of important compounds in the fields such as food control, environmental and clinical analysis. The oxidation of NADH serves as the anodic signal and regenerates the NAD^+ cofactor. However, the oxidation of NADH at conventional solid electrode surface is highly irreversible and takes place at

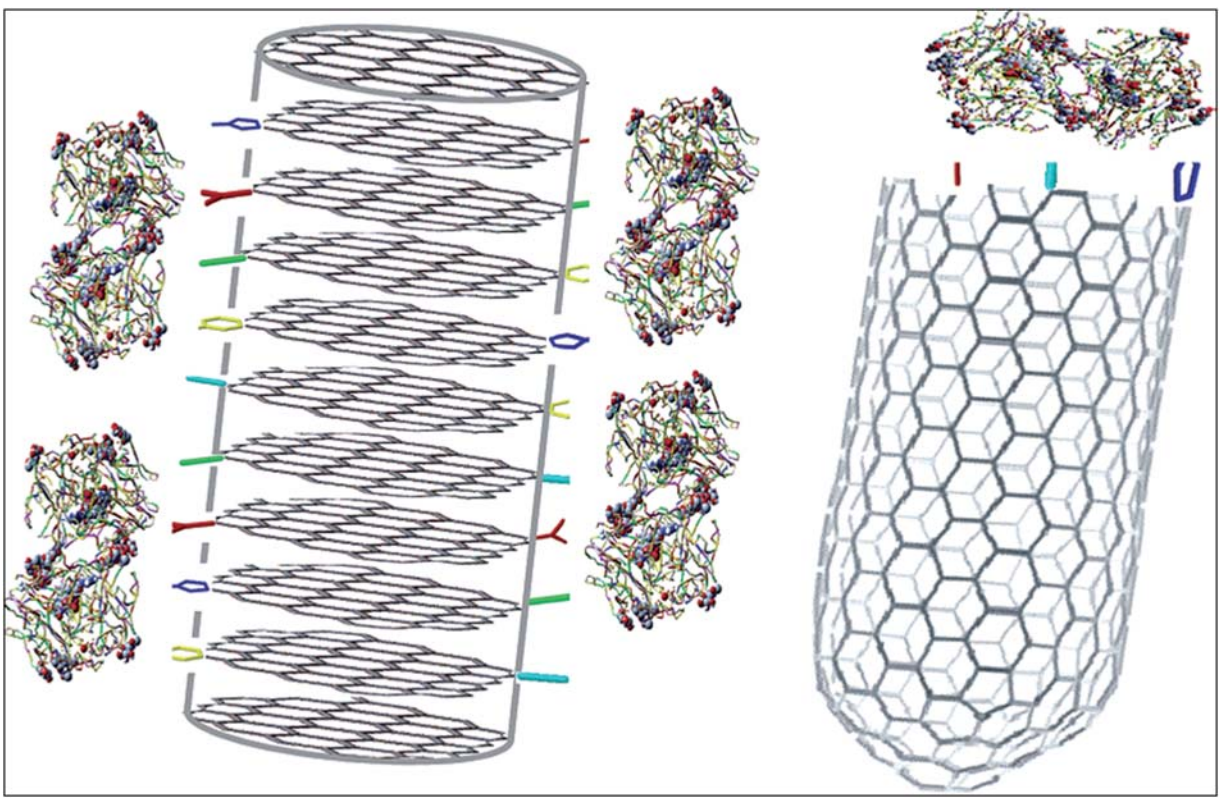

Fig. 5 Schematic picture of the immobilization of the model enzyme GOx on carbon nanofibers and single-walled carbon nanotubes (reproduced with permission from Ref. [9]).

a considerable overpotential, which limits the selectivity of the determination in a real sample.[37] The accumulation of oxidation products at electrode surface also results in severe fouling effect. CNF-modified electrodes are particularly useful for addressing these problems because they can offer improved electron-transfer kinetics, minimized surface fouling and decreased overpotential for NADH oxidation.[20] As shown in Fig. 6A, the CNF-modified electrode exhibited a substantial negative shift of the anodic peak potential by 573 mV and a two times increased peak current, indicating high electrocatalytic activity toward the oxidation of NADH. The CNF-modified electrode allowed highly sensitive amperometric detection of NADH with a low limit of detection (0.11 μM) at a low applied potential (+0.06 V). Based on the high catalytic activity of CNF-modified electrode, an ethanol amperometric biosensor was developed by using a simple drop-coating method for the immobilization of alcohol dehydrogenase (ADH). This biosensor showed a linear response to ethanol concentration over the range of 10 to 425 μM with a detection limit of 3.0 μM (Fig. 6B).

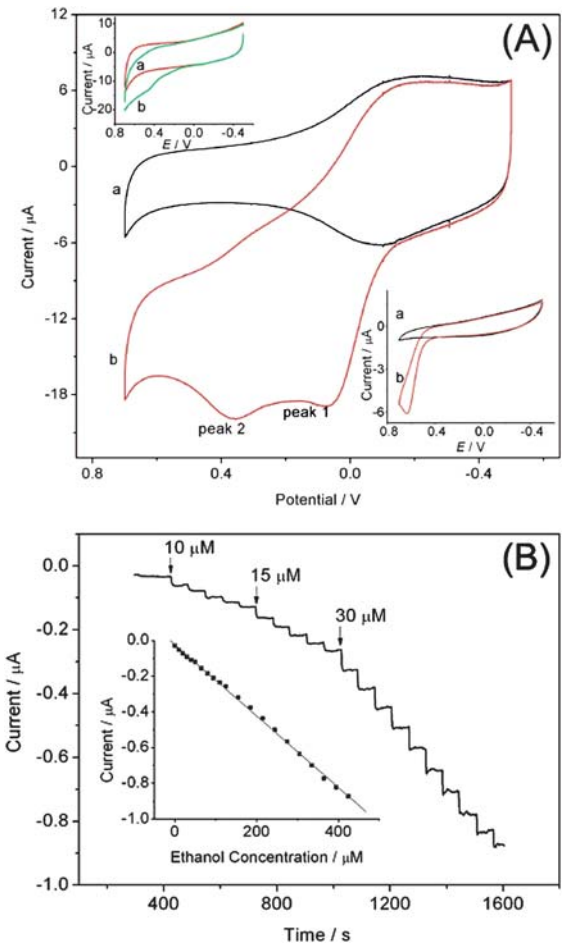

Fig. 6 (A) Cyclic voltammograms of CNF-modified electrode in (a) 0.2 M pH 7.0 PBS and (b) (a) + 2.0 mM NADH. Inset: cyclic voltammograms of bare (lower) and untreated CNF-modified (upper) electrodes in (a) 0.2 M pH 7.0 PBS and (b) (a) + 2.0 mM NADH. Scan rate, 10 mV s^{-1}. (B) Successive amperometric response of the ADH/CNF-modified electrode to ethanol in pH 7.0 PBS at +0.06 V. The ethanol addition each time is from 10, 15, and 30 μM as indicated. Inset shows linear calibration curve (reproduced with permission from Ref. 20).

2.4. CNF-based acetylcholine esterase and tyrosinase biosensors

Vamvakaki and co-workers utilized biomimetically synthesized silica and conductive activated CNFs for the development of a novel electrochemical biosensor system.[38] The enzyme, acetylcholine esterase from *Drosophila melanogaster* (*Dm*. AChE), was directly immobilized onto the CNFs. Subsequently, bioinspired poly(L-lysine) templated silica was grown under mild conditions around the enzyme (Fig. 7). CNFs provided high surface area for the immobilization of enzyme as well as the mediator and transducer for signal monitoring. The initial sensitivity of the silica/nanofiber/AChE biosensor was calculated to be 7.8 μA mM^{-1}. The response of this biosensor was linear to acetylthiocholine concentrations from 0.04 to 0.3 mM. The biosensor presented a remaining activity of 70% after 3.5 months of continuous polarization. Importantly, this silica/nanofiber architecture could improve enzymes stability against thermal denaturation and completely protect them from protease attack. Detailed conformational analysis and rotational mobility of *Dm.* AChE within the poly(L-lysine) templated silica–CNF nanocomposites was conducted by using micro-Raman spectroscopy and electrochemical impedance spectroscopy.[39] Raman analysis confirmed that the enzyme *Dm.* AChE was efficiently encapsulated in silica/nanofiber nanocomposites. From the electrochemical impedance measurements it was concluded that *Dm.* AChE is thermodynamically more stable in the nanocomposites

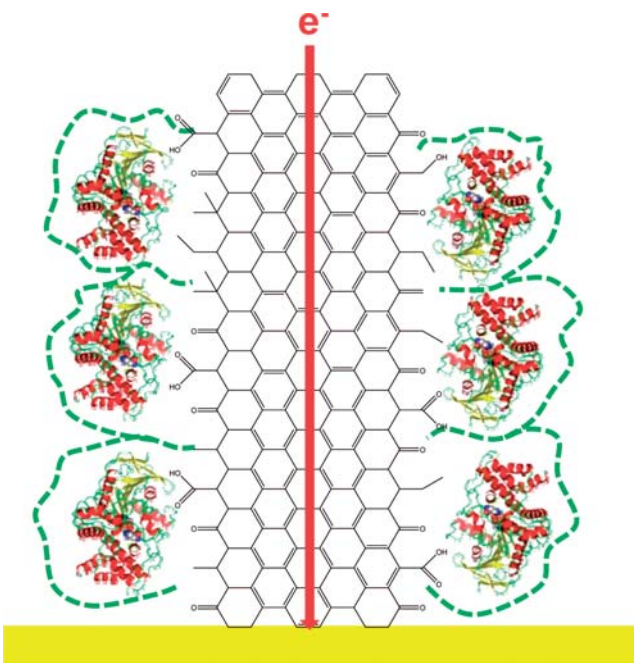

Fig. 7 Schematic representation of the electrochemical silica/nanofiber-based biosensor setup. The dashed green line represents the shield provided by the biomimetically synthesized silica nanostructures. The electron transfer is achieved *via* the conductive CNFs, onto which the active enzyme is immobilized (reproduced with permission from Ref. 38).

with CNFs than the free enzyme. The presence of CNFs in silica/AChE nanocomposites significantly enhanced the analytical characteristics of the amperometric acetylcholine esterase biosensor.

A novel polyaniline–ionic liquid–carbon nanofiber (PANI–IL–CNF) composite film was prepared by *in situ* one-step electropolymerization of aniline in the presence of IL and CNF.[40] By cross-linking tyrosinase to the nanocomposite with glutaraldehyde, a phenol biosensor was further constructed. This architecture combined the advantages of PANI, IL, and CNF makes the immobilized tyrosinase have good affinity to phenolic compounds. The designed biosensors exhibited a wide linear response to catechol ranging from 4.0×10^{-10} to 2.1×10^{-6} M with a high sensitivity of 296 ± 4 A M^{-1} cm^{-2}, a limit of detection down to 0.1 nM at the applied potential of −0.05 V. This biosensor also exhibited highly sensitive amperometric responses to the other phenolic compounds such as *p*-cresol, phenol and *m*-cresol.

2.5 CNF-based immunosensor and cell sensor

Immunoassays are capable of direct and specific detection of clinical, pharmaceutical, biochemical and environmental samples by utilizing the highly specific recognition between antigen and antibody. Compared with conventional ELISA-based immunoassays, immunosensors are of great interest because of their potential utility as specific, simple, label-free and direct detection techniques and the reduction in size, cost and time of analysis.[41] Due to its large functionalized surface area and high surface active groups-to-volume ratio, CNF can be used as ideal immobilization matrix for antigen or antibody to develop immonosensors. Ju's group prepared carcinoma antigen-125 (CA125) immunosensor by covalent binding of CA125 and thionine on a CNF-modified electrode, where thionine was used as the electron-transfer mediator (Fig. 8).[42] The CA125 concentration could be detected based on the electrocatalytic behavior of thionine to the reduction of H_2O_2 catalyzed by labeled HRP due to the formation of immunocomplex on the immunosensor surface after incubation. DPV measurements exhibited a linear response in the concentration range of 2–75 U/ml with a detection limit of 1.8 U/ml ($S\ N^{-1} = 3$).

Ju's group also prepared CNF–chitosan (CS) nanocomposite film for the immobilization and cytosensing of K562 cells on an electrode by the controllable electrodeposition of soluble CNF-doped CS colloidal solution (Fig. 9).[43] This architecture utilized the biocompatibility and good adhesion of CS, and high electric conductivity of CNF. The adhesion of K562 cells on the composite film changed the electron-transfer impedance of the electrochemical probe, thus offering an opportunity for construction of an impedance cell sensor. The CNF acted as an electron conductor for improving electrochemical cytosensing, and could promote electron-transfer reactions between electroactive centers of cells and the electrode. The K562 cell sensor showed a wide linear range of 5.0×10^3 to 5.0×10^7 cells mL^{-1} with a detection limit of 1×10^3 cells mL^{-1}. Very recently, they prepared CNF-doped polypyrrole (ppy) film on indium-tin oxide electrode by electropolymerization method. This highly conductive and biocompatible matrix could be used as both a cell-anchoring substrate and a reporting platform for impedimetric sensing of cell adhesion and proliferation.[44]

2.6 CNF-promoted direct electron transfer of proteins

The study of the direct electron transfer pathways of redox proteins or enzymes is very significant in understanding the redox reaction of proteins, as well as in development of enzyme

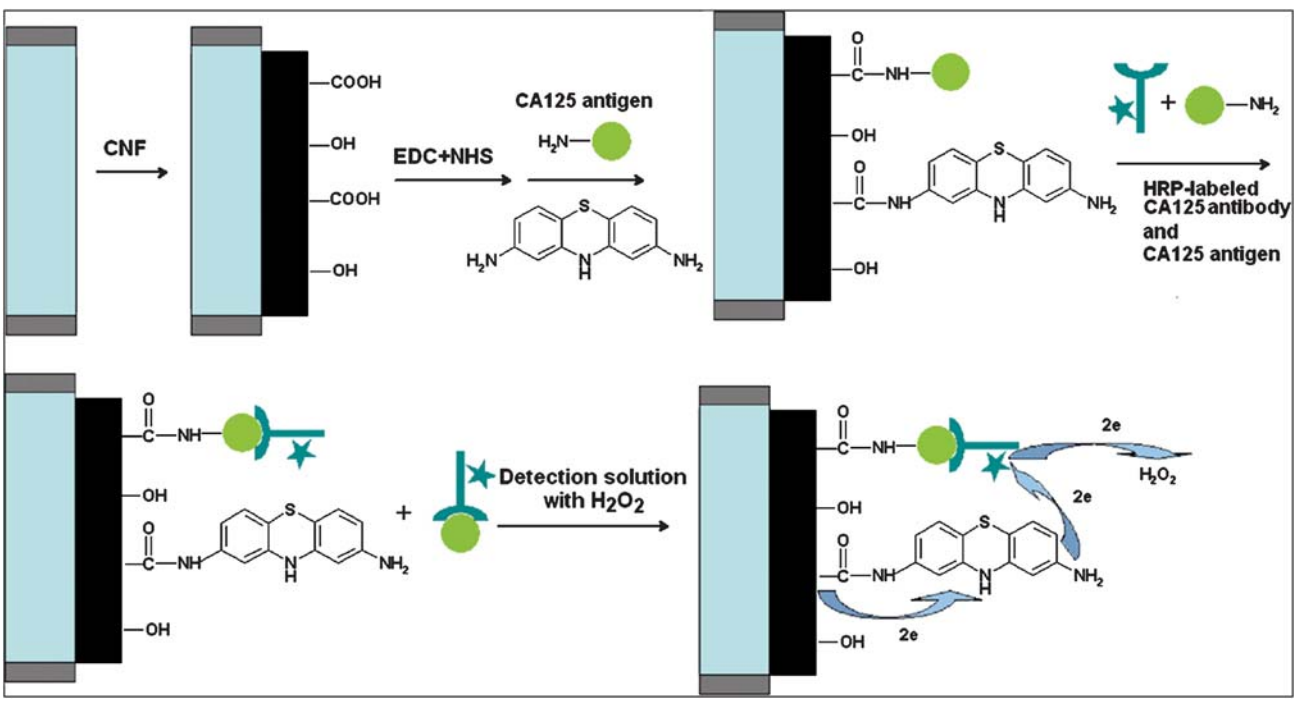

Fig. 8 Preparation and detection procedures of the CA125 immunosensor (reproduced with permission from Ref. 42).

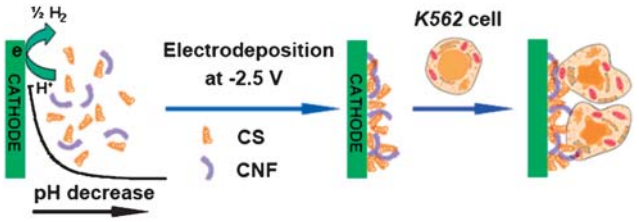

Fig. 9 Preparation of CNF–CS film and impendence sensor for K562 cells (reproduced with permission from Ref. 43).

biosensors. Such direct electrical communication can obviate the need for a co-substrate and allow efficient transduction of the biorecognition event.[4] Since the redox-active center of enzymes and proteins is deeply embedded in its protein shell, direct electron transfer between the protein and the electrode surface has been a great challenge. CNFs can act as nanoscaled electrical wires, just like CNTs,[45] to promote the direct electron transfer between the proteins and the underlying electrode.

For example, CNFs were combined with Nafion to form an organic–inorganic composite, which was used to construct mediator-free hemoglobin (Hb)-based H_2O_2 biosensor.[17] The results revealed that the CNF-based composites could efficiently retain the bioactivity of the entrapped protein. Meanwhile, dramatically facilitated direct electron transfer of Hb and good bioelectrocatalytic activity towards H_2O_2 were demonstrated at the Hb-Nafion-CNF composite film modified glassy carbon electrode. The apparent heterogeneous electron transfer rate constant (k_s) of Hb immobilized on Hb-Nafion-CNF/GC electrode was estimated to be about 2.4 s^{-1}. The prepared H_2O_2 biosensor displayed a wide linear range (1–70 μM), high sensitivity (394 mA cm^{-2} M^{-1}) and low detection limit (0.1 μM). Wu *et al.* observed the direct electrochemistry of alcohol oxidase with the redox potentials of −0.408 V and −0.464 V at CNF–FeTMPyP modified electrode.[36] The results demonstrated that CNF provided a microenvironment for preserving the natural structure and accelerating the electron transfer of the immobilized redox proteins.

3. Vertically aligned carbon nanofiber array as matrix for the immobilization of biomolecules

Vertically aligned carbon nanofibers (VACNFs) can be synthesized in a controlled manner by plasma enhanced chemical vapor deposition (PECVD). Use of the PECVD process allows for control in the size, location, chemical composition, as well as the internal structure of the carbon nanofibers. The nanofibers prepared by this process are grown perpendicularly to the substrate. VACNFs can be grown as individual freestanding structures, or many fibers can be grown in close proximity to each other creating a forest of fibers.[46] This nanostructure provides a bridge between molecular-scale phenomena and the macroscopic world, thereby enabling the realization of truly functional nanoscale devices. Due to the fascinating structural, mechanical, electrical and chemical properties, VACNFs have attracted much attention in electroanalysis as electrode materials or immobilization matrixes for preparation of biosensors. For example, McKnight *et al.* characterized the electrochemical properties of as-grown and treated VACNF forest electrodes with different dimensions.[47] These as-grown electrodes exhibited rapid electron-transfer kinetics with cathodic and anodic peak separations very near the ideal 59 mV for a single electron-transfer reaction, and the anodic/cathodic peak ratio was close to unity.

Due to their high chemical stability, high degree of biologically accessible surface area, vertical orientation, nanoscale dimension, and ease of patterning, VACNFs can be used as interesting substrates for immobilization of biomolecules. For this purpose, several techniques including photochemical grafting of alkenes,[48–50] reaction with diazonium compounds,[48,51,52] "click" chemistry[53] and oxidative methods,[54] have been used to functionalize VACNF surfaces. These functionalized VACNFs provide promising applications in many fields, such as electrochemical and photochemical chemical/biological sensing.

3.1 Covalent modification of VACNFs using photochemical method

Baker and coworkers functionalized VACNFs by reacting them with liquid-phase molecules containing an alkene (C═C) group and inducing the reaction with ultraviolet light (Fig. 10).[48,49] This method could be used to produce different surfaces terminated with primary amines, carboxylic acid groups and alkyl groups. Then thio-modified DNA was covalently linked to the surface of amine group-terminated VACNFs (Fig. 11c).[48] Hybridization studies with complementary and noncomplementary DNA sequences demonstrated this method produced a high density of biomolecular binding sites that exhibited excellent selectivity with a high degree of accessibility. Quantitative measurements showed that VACNFs yielded approximately eight times more hybridized DNA within a given geometric area than planar substrates such as glassy carbon. Furthermore, the DNA-modified VACNFs could be denatured in hot water and rehybridized, demonstrating good chemical stability.

The photochemically functionalized VACNF forests with different terminal groups were also used to immobilize redox-active protein cytochrome *c* (cyt *c*), and the direct electron transfer between cyt *c* and the substrate electrode was studied.[49]

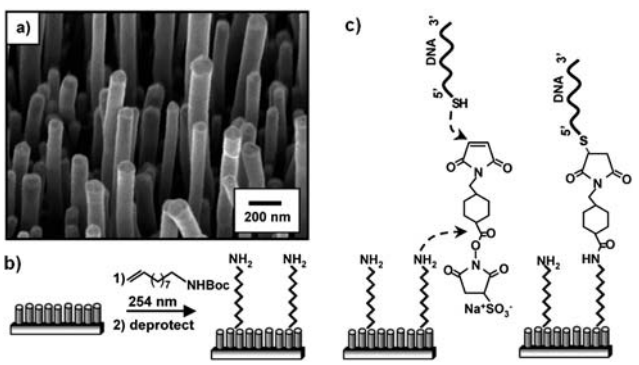

Fig. 10 (a) SEM image (taken at a 25° tilt) of a VACNF substrate. (b) Schematic of photochemical functionalization method to produce amino-terminated surface. (c) Schematic of the method used to covalently link amino-modified VACNFs to thio-modified DNA (reproduced with permission from Ref. 48 and 49).

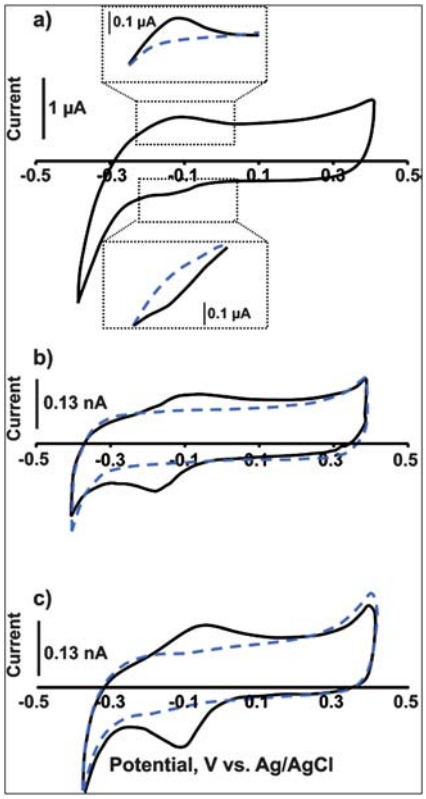

Fig. 11 Cyclic voltammetry of cyt *c* on carboxylic acid-terminated surfaces of (a) VACNF, (b) glassy carbon, and (c) gold electrodes. The solid lines are voltammograms with cyt *c* immobilized onto the electrodes; the dashed lines are background voltammograms taken before cyt *c* was introduced into the cell (reproduced with permission from Ref. 49).

The loading of cyt *c* was measured by using a colorimetric assay based on the oxidation of 2,2′-Azinobis[3-ethylbenzothiazoline-6-sulfonic acid]-diammonium (ABTS) by cyt *c* in the presence of hydrogen peroxide. The data showed that functionalization with carboxylic acid groups led to the highest overall enzymatic activity, while surfaces terminated with neutral (alkane) or positively charged (amine) groups showed much less enzymatic activity. In addition, the VACNFs as matrixes yielded the overall highest activity because of the high biologically accessible surface area. Electrochemical measurements showed that the redox peak separation of cyt *c* was 30–50 mV at VACNF electrode, which was significantly smaller than that obtained at glassy carbon and gold electrode (Fig. 12). This suggested that the nanofiber surface provided unusually good electrochemical reversibility. The peak current due to redox of cyt *c* was approximately 10 times higher on undecylenic acid-modified VACNF surfaces than on undecylenic acid-modified glassy carbon or gold, indicating that the higher surface area of the nanofibers provided 10 times more immobilized cyt *c*. However, the high surface area of nanofibers produced a large increase in capacitive current, which partially obscured the higher signal and decreased the signal-to-noise ratio.

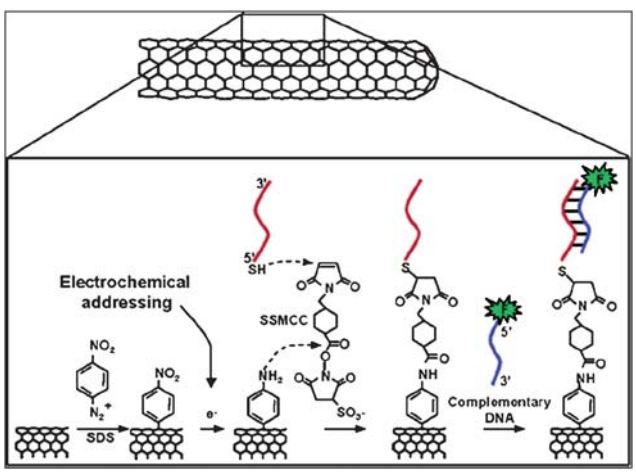

Fig. 12 Schematic illustration of addressable biomolecular functionalization of carbon nanotubes. The procedure for carbon nanofibers is identical (reproduced with permission from Ref. 51).

3.2 Covalent modification of VACNFs *via* diazonium salt chemistry

Another efficient method for the functionalization of VACNFs is based on the reaction of 4-nitrobenzene diazonium tetrafluoroborate salts with nanofiber surfaces, and the nitro groups on the surface can be reduced to primary amines and then linked to biomolecules.[48,51,52]

The electrically addressable biomolecular functionalization of single-walled carbon nanotube (SWNT) electrodes and VACNF electrodes were carried out by Lee and co-workers.[51] The key step of this method is the functionalization of the SWNTs and VACNFs with nitro groups, followed by the "addressable" electrochemical reduction of the nitro groups to amino groups on SWNT and VACNF surface (Fig. 12). The primary amine ($-NH_2$) groups produced by electrochemical reduction are the starting point for covalently linking biomolecules such as DNA, peptides, and antibodies to VACNF surfaces. This research provided a general and direct pathway for fabricating high-density arrays for biosensors using nanoscale components such as nanotubes and nanofibers as immobilization matrixes.

Baker *et al.* studied the difference of photochemical and electrochemical routes for the modification of VACNFs.[48,52] The results demonstrated that both functionalization routes led to DNA-modified surfaces with identical DNA coverage, good selectivity, and good stability. The primary difference between the two functionalization strategies lay in the expected electrical conductivity of the molecular functionalization layer. The aromatic ring connecting the nanofibers to the amine groups is expected to be electrically conductive, while the alkyl chains from the photochemical method are insulating. These discrepancies may make one functionalization method preferable over another for specific applications.

3.3 Modification of VACNFs *via* "click" chemistry

Electrochemically active ferrocene groups could be covalently linked to VACNF surfaces in a simple and efficient manner *via* the Cu(I)-catalyzed azide alkyne cycloaddition (CuAAC), one form of "click" chemistry (Fig. 13).[53] Cyclic voltammetry was used to estimate the number of redox-acitve ferrocene groups on VACNF surfaces, and the density of $(8.8 \pm 0.7) \times 10^{13}$ ferrocene molecules cm^{-2} was obtained. The electrochemical data of

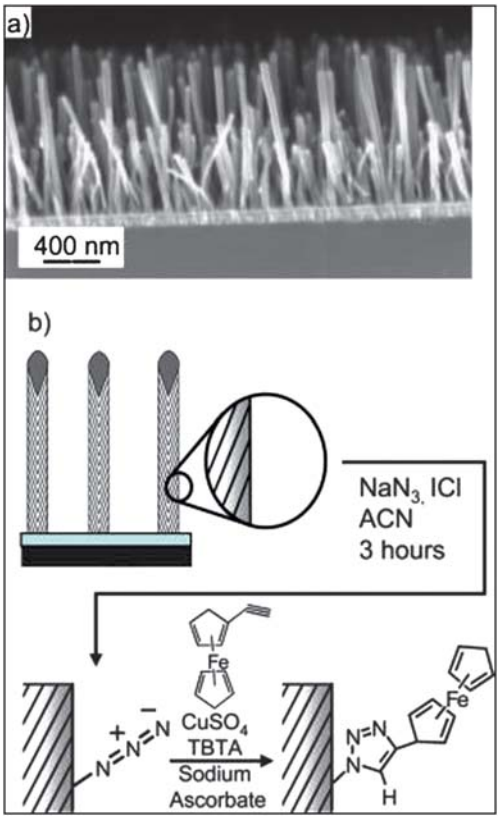

Fig. 13 (a) SEM image of vertically aligned carbon nanofiber cross-section. (b) Reaction scheme of ferrocene attachment to the VACNF surface (reproduced with permission from Ref. 53).

$Fe(CN)_6^{3-/4-}$ redox couple indicated both edge plane and basal-plane sites exist on the surface of nanofibers, and the azido groups likely bind preferentially at the edge-plane sites exposed along the nanofiber sidewalls. The bound ferrocene groups could withstand more than 1500 redox cycles, which suggested that this type of functionalization will find promising use in areas such as electrocatalysis by enabling redox-active or catalytically active molecules to be grafted to nanofibers.

3.4 Other miscellaneous methods for the modification of VACNFs

Fletcher *et al.* reported on two methods for immobilizing biomolecules on the surface of VACNFs.[54] One attachment scheme made use of a kind of heterocyclic aromatic dye compounds to specifically adsorb onto VACNF surfaces. The second scheme involved covalently coupling biomolecules through cross-linking to carboxylic acid sites on the sidewalls of CNFs. Several small molecules and proteins including tetramethylrhodamine, rhodamine-B base, fluorescein, avidin, and streptavidin were studied. The results suggested that the rhodamine based dyes interacted strongly with the VACNFs while fluorescein did not because of the difference of their molecular structures. In contrast to carbon nanotubes, avidin was not found to strongly physisorb to the surface of VACNFs, which was ascribed to the structural difference between carbon nanotubes and VACNFs. In the case of covalent cross-linking procedures, VACNFs were exposed to oxygen plasma for 30 s to produce the abundance of carboxylic acid groups. Both DNA and proteins could be immobilized by coupling pendant amine groups to the exposed carboxylic acid residues on the VACNF surfaces. The immobilization process did not adversely impact the chemical activity of biomolecules.

Weeks *et al.* constructed a reagentless amperometric enzymatic biosensor for detection of ethanol.[55] Yeast alcohol dehydrogenase (YADH) and its cofactor NAD^+ were immobilized by adsorption and covalent attachment to the VACNFs electrode substrate. The technique employed in the covalent process was diimide-activated amidation. The abundance of defect sites on CNFs was not only beneficial for immobilization but also for strong electrical current responses. The linear concentration range of the biosensor with adsorbed enzyme was approximately 1.75 mM to 6 mM ethanol. The linear concentration range of the electrode with covalently immobilized enzyme was approximately 2 mM to 8 mM ethanol.

4. Conclusions

This review has presented recent advances in the application of CNFs for electrochemical biosensing. The attractive properties of CNFs, especially the large amount of edge-plane sites and the high surface active group-to-volume ratio, have paved the way for the construction of a wide range of electrochemical biosensors with excellent analytical performance. The high electrocatalytic activity towards hydrogen peroxide and NADH permitted effective low-potential amperometric biosensing of numerous important substrates. The accelerated electron-transfer kinetics reduced the formation of electrode surface fouling and hence improved the operational stability. Using CNFs as immobilization matrixes, various oxidase, dehydrogenase and other enzyme-based biosensors have been successfully constructed. These biosensors exhibited high sensitivity, and the enzymatic activity was efficiently maintained. The use of CNF molecular wires promoted the direct electron transfer from electrode surfaces to the redox sites of enzymes. VACNF substrates could be effectively functionalized with biomolecules such as DNA and protein through either a photochemical route or by a combined chemical and electrochemical route. These molecular functionalization of VACNFs yielded structures with excellent chemical and biological properties, making them very useful for applications such as chemical sensing/biosensing.

Acknowledgements

The financial support of the National Natural Science Foundation of China (NSFC) is gratefully appreciated (20605020, 20875085). Moreover, the authors gratefully acknowledge financial support from the Foundation of Distinguished Young Scholars of Jilin Province (20060112) and Chinese Academy of Sciences (KJCX2-YW-H11).

References

1 G. M. Swain, In *Handbook of Electrochemistry*, ed. Zoski, C. G., Elsevier, Oxford, 2007, (Chapter 5), p 114.
2 S. Iijima, *Nature*, 1991, **354**, 56–58.

3 Y. P. Sun, K. Fu, Y. Lin and W. J. Huang, *Acc. Chem. Res.*, 2002, **35**, 1096–1104.
4 J. Wang, *Electroanalysis*, 2005, **17**, 7–14.
5 D. Tasis, N. Tagmatarchis, A. Bianco and M. Prato, *Chem. Rev.*, 2006, **106**, 1105–1136.
6 G. G. Wildgoose, C. E. Banks, H. C. Leventis and R. G. Compton, *Microchim. Acta*, 2006, **152**, 187–214.
7 J. Wang and Y. H. Lin, *TrAC, Trends Anal. Chem.*, 2008, **27**, 619–626.
8 P. Serp, M. Corrias and P. Kalck, *Appl. Catal., A*, 2003, **253**, 337–358.
9 V. Vamvakaki, K. Tsagaraki and N. Chaniotakis, *Anal. Chem.*, 2006, **78**, 5538–5542.
10 S.-U. Kim and K.-H. Lee, *Chem. Phys. Lett.*, 2004, **400**, 253–257.
11 C. E. Banks and R. G. Compton, *Analyst*, 2005, **130**, 1232–1239.
12 S. Maldonado and K. J. Stevenson, *J. Phys. Chem. B*, 2004, **108**, 11375–11383.
13 C. A. Bessel, K. Laubernds, N. M. Rodriguez and R. T. K. Baker, *J. Phys. Chem. B*, 2001, **105**, 1115–1118.
14 D. J. Browning, M. L. Gerrard, J. B. Lakeman, I. M. Mellor, R. J. Mortimer and M. C. Turpin, *Nano Lett.*, 2002, **2**, 201–205.
15 I. C. Finegan, G. G. Tibbetts, D. G. Glasgow, J. M. Ting and M. L. Lake, *J. Mater. Sci.*, 2003, **38**, 3485–3490.
16 H. Cui, S. V. Kalinin, X. Yang and D. H. Lowndes, *Nano Lett.*, 2004, **4**, 2157–2161.
17 X. B. Lu, J. H. Zhou, W. Lu, Q. Liu and J. H. Li, *Biosens. Bioelectron.*, 2008, **23**, 1236–1243.
18 L. Wu, X. J. Zhang and H. X. Ju, *Analyst*, 2007, **132**, 406–408.
19 L. Wu, X. J. Zhang and H. X. Ju, *Biosens. Bioelectron.*, 2007, **23**, 479–484.
20 L. Wu, X. J. Zhang and H. X. Ju, *Anal. Chem.*, 2007, **79**, 453–458.
21 Y. Liu, H. Teng, H. Q. Hou and T. Y. You, *Biosens. Bioelectron.*, 2009, **24**, 3329–3334.
22 N. Van Dijk, S. Fletcher, C. E. Madden and F. Marken, *Analyst*, 2001, **126**, 1878–1881.
23 F. Marken, M. L. Gerrard, I. M. Mellor, R. J. Mortimer, C. E. Madden, S. Fletcher, K. Holt, J. S. Foord, R. H. Dahm and F. Page, *Electrochem. Commun.*, 2001, **3**, 177–180.
24 M. A. Murphy, F. Marken and J. Mocak, *Electrochim. Acta*, 2003, **48**, 3411–3417.
25 M. A. Murphy, G. D. Wilcox, R. H. Dahm and F. Marken, *Electrochem. Commun.*, 2003, **5**, 51–55.
26 L. Rassaei, M. Sillanpää, M. J. Bonné and F. Marken, *Electroanalysis*, 2007, **19**, 1461–1466.
27 S. Maldonado and K. J. Stevenson, *J. Phys. Chem. B*, 2005, **109**, 4707–4716.
28 A. Arvinte, F. Valentini, A. Radoi, F. Arduini, E. Tamburri, L. Rotariu, G. Palleschi and C. Balaa, *Electroanalysis*, 2007, **19**, 1455–1459.
29 V. Vamvakaki and N. A. Chaniotakis, *Sens. Actuators, B*, 2007, **126**, 193–197.
30 Z. Z. Li, X. L. Cui, J. S. Zheng, Q. F. Wang and Y. H. Lin, *Anal. Chim. Acta*, 2007, **597**, 238–244.
31 Y. Liu, H. Q. Hou and T. Y. You, *Electroanalysis*, 2008, **20**, 1708–1713.
32 Y. Liu, J. S. Huang, H. Q. Hou and T. Y. You, *Electrochem. Commun.*, 2008, **10**, 1431–1434.
33 J. S. Huang, D. W. Wang, H. Q. Hou and T. Y. You, *Adv. Funct. Mater.*, 2008, **18**, 441–448.
34 J. S. Huang, Y. Liu, H. Q. Hou and T. Y. You, *Biosens. Bioelectron.*, 2008, **24**, 632–637.
35 L. Wu, M. McIntosh, X. J. Zhang and H. X. Ju, *Talanta*, 2007, **74**, 387–392.
36 L. Wu, J. P. Lei, X. J. Zhang and H. X. Ju, *Biosens. Bioelectron.*, 2008, **24**, 644–649.
37 B. A. Deore and M. S. Freund, *Chem. Mater.*, 2005, **17**, 2918–2923.
38 V. Vamvakaki, M. Hatzimarinaki and N. A. Chaniotakis, *Anal. Chem.*, 2008, **80**, 5970–5975.
39 M. Hatzimarinaki, V. Vamvakaki and N. A. Chaniotakis, *J. Mater. Chem.*, 2009, **19**, 428–433.
40 J. Zhang, J. P. Lei, Y. Y. Liu, J. W. Zhao and H. X. Ju, *Biosens. Bioelectron.*, 2009, **24**, 1858–1863.
41 T. Hianik, M. Šnejdárková, L. Sokolíková, E. Meszár, R. Krivánek, V. Tvarožek, I. Novotný and J. Wang, *Sens. Actuators, B*, 1999, **57**, 201–212.
42 L. Wu, F. Yan and H. X. Ju, *J. Immunol. Methods*, 2007, **322**, 12–19.
43 C. Hao, L. Ding, X. J. Zhang and H. X. Ju, *Anal. Chem.*, 2007, **79**, 4442–4447.
44 L. Ding, C. Hao, X. J. Zhang and H. X. Ju, *Electrochem. Commun.*, 2009, **11**, 760–763.
45 F. Patolsky, Y. Weizmann and I. Willner, *Angew. Chem., Int. Ed.*, 2004, **43**, 2113–2117.
46 A. V. Melechko, V. I. Merkulov, T. E. McKnight, M. A. Guillorn, K. L. Klein, D. H. Lowndes and M. L. Simpson, *J. Appl. Phys.*, 2005, **97**, 041301, Art. No. 041301.
47 T. E. McKnight, A. V. Melechko, M. A. Guillorn, V. I. Merkulov, M. J. Doktycz, C. T. Culbertson, S. C. Jacobson, D. H. Lowndes and M. L. Simpson, *J. Phys. Chem. B*, 2003, **107**, 10722–10728.
48 S. E. Baker, K.-Y. Tse, E. Hindin, B. M. Nichols, T. L. Clare and R. J. Hamers, *Chem. Mater.*, 2005, **17**, 4971–4978.
49 S. E. Baker, P. E. Colavita, K.-Y. Tse and R. J. Hamers, *Chem. Mater.*, 2006, **18**, 4415–4422.
50 E. C. Landis and R. J. Hamers, *J. Phys. Chem. C*, 2008, **112**, 16910–16918.
51 C.-S. Lee, S. E. Baker, M. S. Marcus, W. Yang, M. A. Eriksson and R. J. Hamers, *Nano Lett.*, 2004, **4**, 1713–1716.
52 S. E. Baker, K.-Y. Tse, C.-S. Lee and R. J. Hamers, *Diamond Relat. Mater.*, 2006, **15**, 433–439.
53 E. C. Landis and R. J. Hamers, *Chem. Mater.*, 2009, **21**, 724–730.
54 B. L. Fletcher, T. E. McKnight, A. V. Melechko, M. L. Simpson and M. J. Doktycz, *Nanotechnology*, 2006, **17**, 2032–2039.
55 M. L. Weeks, T. Rahman, P. D. Frymier, S. K. Islam and T. E. McKnight, *Sens. Actuators, B*, 2008, **133**, 53–59.